Est. 1984

Structural Analysis of LiNi$_x$Mn$_{2-x}$O$_4$ Prepared by Irradiation Microwave-Assisted Reflux Technique

DYAH PURWANINGSIH*, HARI SUTRISNO and HARYO ROHMADIYANTO

Department of Chemistry Education, Faculty of Mathematics and Natural Sciences,
Yogyakarta State University, Jl. Colombo 1, Yogyakarta 55281, Indonesia.
*Corresponding author E-mail: dyah_purwaningsih@uny.ac.id

ABSTRACT

This study aims to synthesize Ni-doped LiNi$_x$Mn$_{2-x}$O$_4$ (x = 0, 0.02, 0.04, 0.06, 0.08, 0.1) by irradiation microwave-assisted reflux technique. The microstructure of the products was investigated by x-ray diffraction equipped with U-FIT program package. Results of the structural analysis show that Ni doping changed the size, crystallinity, and microstructure of LiNi$_x$Mn$_{2-x}$O$_4$. The LiNi$_x$Mn$_{2-x}$O$_4$ solids have a cubic structure with a space group of Fd^{-3} m. Increasing the content of Ni doping does not affect the structure. The average volume of LiNi$_x$Mn$_{2-x}$O$_4$ is around 555 Å3 to 580 Å3. The crystallinity of the solids tends to increase with the increasing Ni content accompanied by the decrease in unit cell lattice parameters.

Keywords: LiNi$_x$Mn$_{2-x}$O$_4$, Mole ratio of Ni/Mn, Irradiation microwave-assisted reflux technique, Microstructure.

INTRODUCTION

In the current era, innovations in the field of technology have been rapidly increased. One is the electronic portable items such as mobile phones, laptops, cameras, hybrid cars, and others. Battery as a power source was instrumental component in the technological innovation. One type of the power source is a lithium battery. Currently, the common source of lithium is LiCoO$_2$ that widely used as a cathode material for lithium-ion batteries. However, LiCoO$_2$ has several disadvantages which are difficult to be used as a large-sized cathode material, security issues in high power and high cost. This has an impact on the amount of research that focus on the development of other alternative cathode material in view of cost, safety and environment issues[1,2].

Although many new cathode materials have been developed, LiMn$_2$O$_4$ is recognized as a promising alternative positive electrode for lithium-ion batteries[3]. Spinel structure of LiMn$_2$O$_4$ offers an attractive alternative material beyond LiCoO$_2$ available commercially. The advantages of using LiMn$_2$O$_4$ are that materials are safe, non-toxic, and low cost[4].

However, $LiMn_2O_4$ has a constraint of life-time, being reduced levels of storage capacity in applications[5]. The biggest constraint is the life-time at high temperature. This happens because of the dissolution of manganese into the electrolyte which is then followed by the disproportionation of Mn^{3+} ions, the decomposition of the electrolyte, and changes in the structure of the powder particles after Jahn-Teller distortion in the cells that consume the battery content[6]. These constraints can be reduced by other transition metals having structural conformity to give $LiNi_xMn_{2-x}O_4$ where M = Co, Mg, Al, Cr, Ni, Fe, Ti and Zn[7].

Many methods of synthesis have been reported to prepare $LiMn_2O_4$ compound. These includes sol-gel method[8], hydrothermal[9], spray-pyrolysis[10], and so forth. However, studies related to the synthesis of compounds of $LiNi_xMn_{2-x}O_4$ (x = 0–0.1) are hardly reported, particularly those that deals with the use of irradiation microwave-assisted reflux technique, followed by solid-state reaction.

This paper reports the result of the synthesis of $LiNi_xMn_{2-x}O_4$ (x = 0–0.1) prepared by irradiation-microwave assisted reflux-technique and its microstructural characterization. By using this technique, it is expected that the complex reactions between lithium ion, nickel ion, manganese ion, and citric acid monohydrate (as a charge stabilizer and chelating agents) will occur. Irradiation microwave is used so that the collision among the molecules occur more rapidly and therefore the reaction will proceed more easily and efficiently to produce the manganese oxide. Hence, the solid-state reaction was used to lithiation process and doping nickel metal in oxide manganese compounds with the chelating agent. The effects of various mole ratio of Ni/Mn in the synthesis of the products are structurally reported in detail in this work.

MATERIALS AND METHODS

Synthesis of Mn_2O_3 and $LiNi_xMn_{2-x}O_4$
Analytical grade of $Mn(CH_3COO)_2 \cdot 4H_2O$ and $Na_2S_2O_8$ (E.Merck) has been used. All other chemicals used without further purification. In a typical synthesis, $Mn(CH_3COO)_2 \cdot 4H_2O$ and $Na_2S_2O_8$ with a mole ratio of 1:1 was dissolved at room temperature in 80 mL of deionized distilled water. The mixture was stirred to form a homogeneous solution.

The solution was refluxed with the aid of irradiation microwave intensity of 50% of 760 watts for 20 minutes. The precipitate obtained was separated and dried at 250°C for 1 h in an oven and calcination at 750°C for two hours.

Synthesis $LiNi_xMn_{2-x}O_4$ is as follows; one-mole LiOH, 0.02 mol of $Ni(CH_3COO)_2 \cdot 4H_2O$, and 1.98 mol of Mn_2O_3 synthesized, dispersed into citric acid monohydrate to form a thick slurry. It was dried in the oven at 250°C for one hour. Solids of $LiNi_{0.02}Mn_{1.98}O_4$ then was calcined at 750°C for two hours. The same procedure was carried out to synthesize materials with different mole ratios.

Determination and Characterization of $LiNi_xMn_{2-x}O_4$
Powder Mn_2O_3 and $LiNi_xMn_{2-x}O_4$ were analyzed using X-Ray Diffractometer. The XRD pattern obtained in XRD instrument Rigaku Miniflex 600-Benchtop using CuKα radiation (λ = 1.5406 Å) at room temperature. XRD instrument was set to operate at 40 kV and 15 mA. XRD data obtained by 2θ interval ranging from 20° to 80°. Rietveld analysis was performed with the software package U-FIT to refine X-ray diffraction data. The parameters for refining are a unit cell, hkl, and volume. SEM image was obtained using a JEOL JSM-6510LASEM. Effect of nickel content on the structure of $LiMn_2O_4$ was studied using Energy Dispersive X-ray spectroscopy. EDX analysis is also used to analyze the presence of Mn, O_2 and Ni elements in material prepared.

RESULTS AND DISCUSSION

XRD Patterns
Figure 1 shows the XRD generated pattern of $LiNi_xMn_{2-x}O_4$. High peak intensity indicates that the $LiNi_xMn_{2-x}O_4$ has a good crystallinity. Fig. 2 shows the variation of lattice constants of materials with different compositions. The refinement data obtained using the U-FIT indicates that the lattice parameter decreases with increase in doping content.

Replacement Mn^{3+} by Ni^{2+} in the octahedral site (16d) causes a decrease in the lattice parameter, while the lithium ions occupy tetrahedral sites (8a). After modification, lattice shrinkage caused by smaller ionic radius of Ni^{2+} which replaces the Mn^{3+} sites in 16d. Note that the ionic radius of Ni^{2+} of 0.560 Å is smaller than that of Mn^{3+}, which is 0.645 Å. The

differences in the ionic radius between Ni^{2+} and Mn^{3+} is relatively small, therefore only a view of changing the lattice parameters is observed. On the other hand, the replacement of Mn^{3+} by Ni^{2+} induces the increase of the content of Mn^{4+} to maintain the balance of the refill process (charge), since Mn^{4+} has an ionic radius smaller than the Mn^{3+}, this also contribute to lattice shrinkage. Oxygen atoms are arranged in a hermetically sealed packaging 32e[11,12].
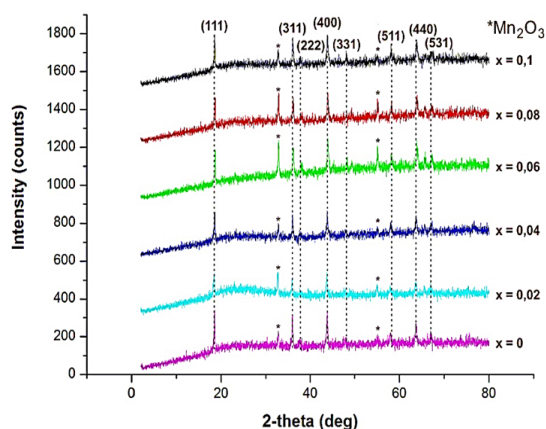

Fig. 1. XRD pattern of $LiNi_xMn_{2-x}O_4$

Table 1 shows the areas hkl various mole ratio of Ni/Mn in $LiNi_xMn_{2-x}O_4$ using U-FIT program. The products have a cubic phase with space group Fd-3m as shown by the results of the analysis using the U-FIT program in Table 2. There was no significant difference in the crystal structure after it is being doped. It shows that the Mn sites in $LiMn_2O_4$ are replaced completely by Ni, although there are other phases of Mn_2O_3 are formed. The emergence of this phase of Mn_2O_3 may be due to the availability of the rest of Mn_2O_3 which is not completely reacted with LiOH in the lithiation process. This phase is shown by the peak area of 32–33° and 54–55° attributed to Mn_2O_3.

Figure 3 shows the SEM-EDX Mn_2O_3, $LiMn_2O_4$, and the $LiNi_{0.08}Mn_{1.92}O4$. Based on the SEM image it can be seen that in general the three samples showing the non- homogeneous particle surface. Qualitatively, it appears that the particles forms agglomeration. It is indicated by the structure of particles that joined by each other compatibly, so that the grain/single particles do not appear clearly. It is noteworthy that the shape of the particle is basically irregular cubic.

Table 1: Fields hkl of $LiNi_xMn_{2-x}O_4$

| $LiNi_xMn_{2-x}O_4$	Lattice Parametersa = b = c (Å)	Space Group	Crystal Volume(Å³)	Figure of Merite	
				D	R
$LiMn_2O_4$	8.28383	Fd-3m	568.4941	0.0237	0.0428
$LiNi_{0.02}Mn_{1.98}O_4$	8.27991	Fd-3m	567.7973	0.0466	0.0792
$LiNi_{0.04}Mn_{1.96}O_4$	8.26919	Fd-3m	565.4537	0.0294	0.0539
$LiNi_{0.06}Mn_{1.94}O_4$	8.33935	Fd-3m	579.9954	0.0307	0.0692
$LiNi_{0.08}Mn_{1.92}O_4$	8.21942	Fd-3m	555.0103	0.0187	0.0345
$LiNi_{0.1}Mn_{1.9}O_4$	8.25553	Fd-3m	562.6390	0.0224	0.0402
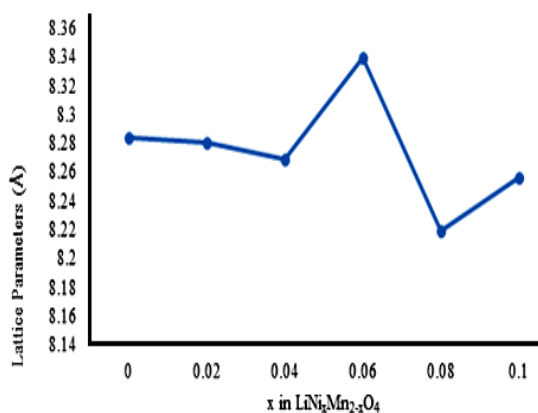
Fig. 2. Variation of lattice parameters with x in $LiNi_xMn_{2-x}O_4$

The average particle size of the nickel-doped samples is smaller than that of undoped $LiMn_2O_4$. The doping of $LiNi_xMn_{2-x}O_4$ with Ni causes the tendency of nucleation process and hinder the formation of crystal growth. The Ni-doped $LiMn_2O_4$ powders have irregular particle size. The increase in the nickel doping leads to increase in $LiMn_2O_4$ particle size. The morphology is almost similar[11].

As expected, the EDX data of the materials show the Ni content in accordance with the predetermined Ni to Mn molar ratio. It suggests that the Ni content in the $LiMn_2O_4$ corresponds to the amount of Mn in the structure that has been replaced. Also, it is also clearly observed the peak intensity of Ni increases with an increase in Ni content, as expected.

**Table 2: Results of analysis using the U-FIT program**

mx = 0		x = 0.02		x = 0.04		x = 0.06		x = 0.08		x = 0.1		hkl
2θ	I/Io	2θ	I/Io	2θ	I/Io	2θ	I/Io	2θ	I/Io	2θ	I/Io	
18.649	100	18.463	81	18.556	95	18.623	87	18.591	90	18.531	100	111
35.973	87	35.884	66	36.038	84	36.135	77	36.112	84	36.095	85	311
37.717	7	-	-	37.622	16	37.851	30	37.837	30	37.834	21	222
43.803	96	43.705	100	43.818	100	43.935	94	43.912	97	43.91	92	400
47.949	23	47.88	25	48.042	22	48.14	32	48.098	38	48.067	38	331
58.012	30	57.967	29	58.104	39	58.136	31	58.136	53	58.104	57	511
63.738	56	63.705	44	63.755	60	-	-	63.928	58	63.871	59	440
67.109	14	67.004	36	67.07	31	-	-	67.203	29	67.2	23	531
75.539	4	75.307	31	-	-	75.52	23	-	-	75.608	23	533
-	-	-	-	76.631	30	76.381	15	76.767	23	76.612	18	622
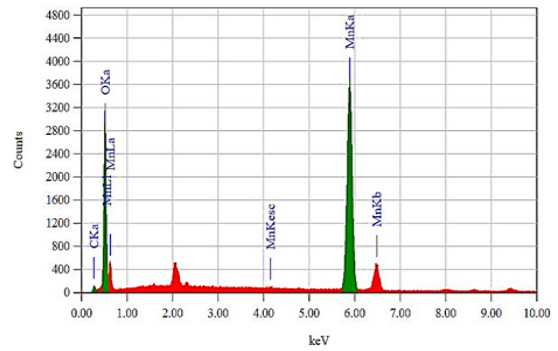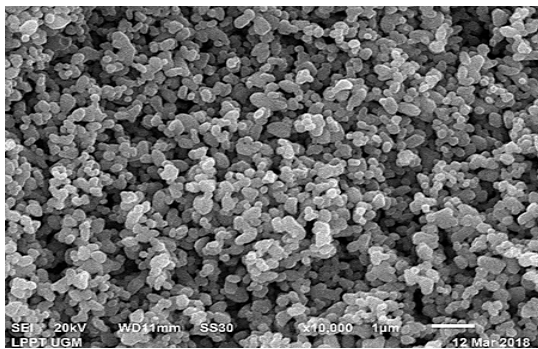
(a)
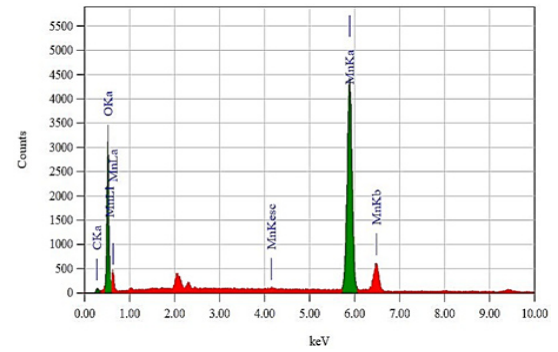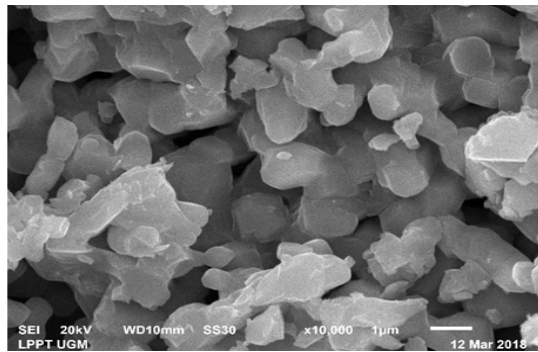
(b)
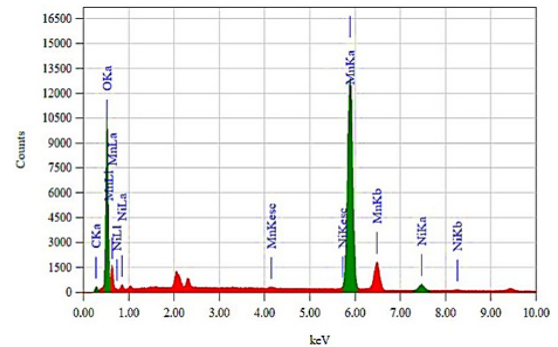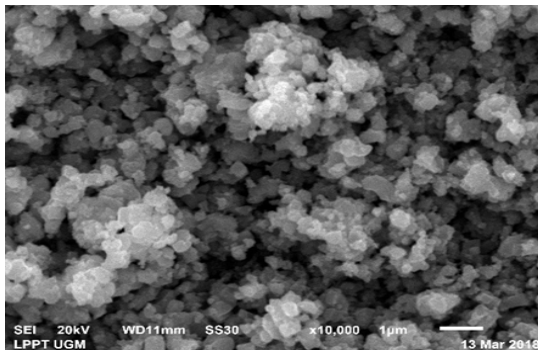
(c)

Fig. 3. SEM-EDX of (a) Mn_2O_3 (b) $LiMn_2O_4$ and (c) the $LiNi_{0.08}Mn_{1.92}O_4$

CONCLUSION

It has been shown that $LiNi_xMn_{2-x}O_4$ has successfully been synthesized by using irradiation microwave-assisted reflux technique. The $LiNi_xMn_{2-x}O_4$ powders have a cubic crystal structure with an $Fd^{-3}m$ space group. The particle size of the prepared materials is not homogeneous. Doping with Ni leads to change in size, crystallinity, and microstructure of the product. The average volume of $LiNi_xMn_{2-x}O_4$ is about 555 Å3 to 580 Å3. The crystallinity of the materials tends to increase with the increase in the Ni doping content. On the other hand, the lattice parameter decreases with the increase of Ni content. The synthesized $LiNi_xMn_{2-x}O_4$ has been expected to give a better performance as a lithium-ion battery's cathode.

REFERENCES

1. Chebiam, R.V.; Prado, F; Manthiram, A.; *Chem. Matter.*, **2001**, *13*, 2951–2957.
2. Venkatraman, S.; Shin, Y.; Manthiram, A.; *Electrochem. Solid-State Lett.*, **2003**, *6*, A9–A12.
3. Fergus, J. W.; *J. Power Sources.*, **2010**, *195*, 939–954.
4. Julien, C. M.; Mauger, A.; Zaghib, K.; Groult, H., *Inorganics.*, **2014**, *2*, 132–154
5. Hu, M.; Pang, X.; Zhou, Z., *J. Power Sources.*, **2013**, *237*, 229–242.
6. Gabrisch, H.; Ozawa, Y.; Yazami, R., *Electrochim. Acta.*, **2006**, *52*, 1499–1506.
7. Peng, C., Bai, H., Xiang, M., Su, C.; Liu, G.; Guo, J., *Int. J. Electrochem. Sci.*, **2014**, *9*, 1791–1798.
8. Michalska, M.; Lipinska, L.; Mirkowska, M.; Aksienionek, M., Diduszko, R.; Wasiucionek, M., *Solid State Ionics.*, **2011**, *188*, 160–164.
9. Yue, H. J.; Huang, X. K.; Lv, D. P.; Yang, Y., *Electrochim. Acta.*, **2009**, *54*, 5363–5367.
10. Iriyama, Y.; Tachibana, Y.; Sasasoka, R.; Kuwata, N.; Abe, T.; Inaba, M.; Tasaka, A.; Kikuchi, A.; Kawamura, J.; Ogumi, Z., *J. Power Sources.*, **2007**, *174*, 1057–1062.
11. Purwaningsih, D.; Roto, R.; Sutrisno, H., *IOP Conf.*, **2014**, *107*, 1–8.
12. Li, X.; Xu, Y.; Wang, C., *J. Alloys Compd.*, **2009**, *479,* 310–313.